Anal. Chem. **2006,** *78,* 7870−7876

High-Throughput Positive-Dielectrophoretic Bioparticle Microconcentrator

Nitzan Gadish and Joel Voldman*

Department of Electrical and Computer Science, Massachusetts Institute of Technology, 77 Massachusetts Avenue, Building 36-854, Cambridge, Massachusetts 02139

We introduce a new dielectrophoretic particle microconcentrator that combines interdigitated electrodes with a chaotic mixer to achieve high-throughput (>100 μL/min) particle concentration. The interdigitated electrodes use positive dielectrophoresis to attract particles to the surface, while the chaotic mixer circulates the particles to increase the number brought in proximity with the surface. We have used this microconcentrator to concentrate both beads and *B. subtilis* spores and have developed a microvolume concentration measurement method to determine the delivered off-chip concentration enhancement of the output sample. The resulting microconcentrator is sufficiently high throughput to serve as an interface between macroscale sample collectors and micro- or nanoscale detectors.

Pathogen sensing is essential in many applications ranging from water quality monitoring[1] to biological warfare agent detection.[2] Among the approaches that exist for pathogen detection, microfluidic devices are especially appropriate as they operate optimally with particles on the micron scale. Many microfluidic pathogen-detecting devices have been created, using principles ranging from molecular detection[3] to direct affinity detection of microorganisms.[4]

Microfluidic concentrators serve as sample preparation subsystems in complete microorganism detection systems. A concentrator works by accumulating the particles of interest from a sample and resuspending them in a smaller volume of solution, resulting in an increased sample concentration. As such, microfluidic concentrators perform two important functions. First, by increasing the concentration of sample presented to the detector, they increase the overall sensitivity of the system. Second, the microconcentrator corrects the volume mismatch between the samples obtained by standard collection methods (∼mL) and the volume most microfluidic devices can process in a reasonable amount of time (∼μL).

Concentration requires selectively applying a force to the particles of interest but not to the liquid in which they are suspended. At the macroscale, common methods of concentration include membrane filtering and centrifugation. At the microscale, several methods exist for concentrating particles. Acoustic microconcentrators have been developed that concentrate particles by focusing them to the nodes or antinodes of standing acoustic waves.[5,6] Membrane filtering has also been performed at the microscale.[7]

An alternative approach to concentrating particles at the microscale is to use electric fields to apply forces to either a charged particle (e.g., electrophoresis) or induced dipoles in the particle. The latter method is known as dielectrophoresis (DEP).[8,9] DEP refers to the force on polarizable particles in a spatially nonuniform electric field and provides a suitable method for manipulating microparticles in liquid suspension. It works optimally with microscale particles and devices, integrating seamlessly with microfluidics. Two types of forces can be exerted: particles can be pulled toward points of maximum electric field (termed positive DEP, or pDEP) or pushed toward locations of minimum electric field (termed negative DEP, or nDEP). Dielectrophoretic forces can be produced using simple planar electrodes, making devices simple to fabricate.[10,11] Moreover, electric fields can be quantitatively modeled, enabling optimization of device design.[12−15] Finally, DEP is an active mechanism that can easily be turned on and off.[16]

Researchers have already developed several DEP concentrators. Zhou et al. created a microconcentrator that used interdigi-

* To whom correspondence should be addressed. E-mail: voldman@mit.edu, Fax: 617-258-5846.

(1) Ford, T. E. *Environ. Health Perspect*, **1999**, *107*, 191−206.
(2) Ivnitski, D.; O'Neil, D. J.; Gattuso, A.; Schlicht, R.; Calidonna, M.; Fisher, R. *Biotechniques* **2003**, *35*, 862−869.
(3) Belgrader, P.; Young, S.; Yuan, B.; Primeau, M.; Christel, L. A.; Pourahmadi, F.; Northrup, M. A. *Anal. Chem.* **2001**, *73*, 286−289.
(4) Pepper, J.; Noring, R.; Klempner, M.; Cunningham, B.; Petrovich, A.; Bousquet, R.; Clapp, C.; Brady, J.; Hugh, B. *Sens. Actuators, B* **2003**, *96*, 565−575.
(5) Nilsson, A.; Petersson, F.; Jonsson, H.; Laurell, T. *Lab Chip* **2004**, *4*, 131−135.
(6) Harris, N. R.; Hill, M.; Beeby, S.; Shen, Y.; White, N. M.; Hawkes, J. J.; Coakley, W. T. *Sens. Actuators, B* **2003**, *95*, 425−434.
(7) Floriano, P. N.; Christodoulides, N.; Romanovicz, D.; Bernard, B.; Simmons, G. W.; Cavell, M.; McDevitt, J. T. *Biosens. Bioelectron.* **2005**, *20*, 2079−2088.
(8) Pethig, R. *Crit. Rev. Biotechnol.* **1996**, *16*, 331−348.
(9) Jones, T. B. *Electromechanics of particles*; Cambridge University Press: Cambridge, 1995.
(10) Huang, Y.; Pethig, R. *Meas. Sci. Technol.* **1991**, *2*, 1142−1146.
(11) Hughes, M. P.; Morgan, H.; Rixon, F. J.; Burt, J. P.; Pethig, R. *Biochim. Biophys. Acta* **1998**, *1425*, 119−126.
(12) Rosenthal, A.; Voldman, J. *Biophys. J.* **2005**, *88*, 2193−2205.
(13) Voldman, J.; Braff, R. A.; Toner, M.; Gray, M. L.; Schmidt, M. A. *Biophys. J.* **2001**, *80*, 531−541.
(14) Voldman, J.; Toner, M.; Gray, M. L.; Schmidt, M. A. *J. Electrost.* **2003**, *57*, 69−90.
(15) Schnelle, T.; Muller, T.; Fuhr, G. *J. Electrost.* **1999**, *46*, 13.
(16) Taff, B. M.; Voldman, J. *Anal. Chem.* **2005**, *77*, 7976−7983.

10.1021/ac061170i CCC: $33.50
Published on Web 10/19/2006

tated electrodes and insulating beads to concentrate yeast.[17] A team at Sandia National Laboratories, meanwhile, has introduced a concentrator with external electrodes that uses insulating posts to create field nonuniformities[18] and have been able to concentrate *Escherichia coli*, spores and viruses using this device.[19] We have been developing a microconcentrator for detecting spores in water and, in this report, address several outstanding issues in the field. First, we present electrode design rules for optimal particle capture onto interdigitated electrodes, which are one of the most commonly used electrode configurations.[20,21] Second, we use these design rules to create a concentrator able to operate at high throughput (up to 100 μL/min) with actual biological spores. Third, we have measured the concentration enhancement of the device using released concentrate, rather than estimating concentration enhancement on-chip.

Finally, we have incorporated a chaotic mixer into our design that significantly enhances the performance of the concentrator. There is typically a tradeoff between the efficiency of a concentrator and its throughput; operating at higher flow rate makes it more difficult for the DEP capture force to overcome the disrupting fluid drag. Thus, most bacterial concentrators operate in the microliter per hour to microliter per minute flow rate range in order to obtain reasonable efficiency. Prior attempts to increase capture efficiency include, for instance, adding electrodes to both top and bottom of a chamber.[22,23] Our approach is to use a chaotic mixer to increase capture efficiency. First introduced by Stroock et al.,[24] this mixer contains angled grooves at the top of the channel that preferentially lower the fluid resistance along the groove, generating flows transverse to the main flow direction (e.g., circulating flows). By suitably arranging the grooves, one is able to repeatedly circulate and intermix two fluids, resulting in chaotic mixing that brings outlying particles close to the electrodes for capture. Together these developments serve to move microscale concentrators closer to deployment.

MATERIALS AND METHODS

Beads. We purchased 1-μm-diameter carboxyl-modified magnetic fluorescent pink polystyrene microspheres from Spherotech, Inc. (Libertyville, IL) in 1% w/v suspension (1.21×10^{10} beads/mL). We occasionally used these beads as test particles for characterization experiments in place of spores. We resuspended beads at 200×, 20000×, and 40000× dilutions in deionized water resulting in concentrations of 6×10^7, 6×10^5, and 3×10^5 beads/mL, respectively. We measured suspension conductivities to be $\sim 5 \times 10^{-4}$ S/m using a Thermo Orion model 555A conductivity meter (VWR, Cambridge, MA).

Spores. We purchased *Bacillus subtilis* spores (ATCC 6633) suspended in deionized water at a concentration of 3.8×10^8 cfu/mL from Raven Biological Laboratories, Inc. (Omaha, NE). We stained spores with 190 μg/mL concanavalin A–AlexaFluor 488 conjugate (C11252, Invitrogen, Carlsbad, CA) overnight at 4 °C. We washed stained spores 3× with deionized water and then resuspended at a 100× dilution in deionized water resulting in a final concentration of 3.8×10^6 cfu/mL.

Device Fabrication. We patterned 200-nm-thick gold (with 10-nm Ti adhesion layer) interdigitated electrodes on 6-in.-diameter Pyrex substrates (Bullen Ultrasonics, Eaton, OH) using a standard liftoff process. We created electrodes with both 10- and 25-μm width and spacing. We drilled 0.75-mm-diameter holes using a diamond drill bit (C. R. Laurence Co., Inc., Los Angeles, CA) to provide fluidic access. Each die was dip-coated in a solution of Sylgard Prime Coat (Dow Corning, Midland, MI) diluted 11× in heptane (anhydrous 99%; Sigma-Aldrich, St. Louis, MO). The Prime Coat can be removed by a 4-h soak in 100 mg/mL KOH followed by a short heptane rinse.

We molded PDMS flow chambers using an SU-8 master mold patterned on a silicon wafers. We used a two-level SU-8 process to create the chaotic mixer, involving a 100-μm layer of SU-8 2050 (MicroChem, Newton, MA) and a 50-μm layer of SU-8 2025 (MicroChem). The two layers of SU-8 were developed for ~10 min (visual stop) in PM acetate and then silanized for 2 h in HMDS. A ~3-mm-thick layer of PDMS was poured over the entire wafer and set to cure for 3 h at 65 °C to mold the channels.

Packaging. The device was assembled on a custom-designed PCB (ExpressPCB, Santa Barbara, CA) using a variation of our previously described packaging scheme (Figure 2).[16] Briefly, drilled fluidic access holes in the Pyrex die aligned to corresponding holes in the PCB. The holes were sealed to each other using NanoPort adhesive rings (N-100-01; Upchurch Scientific, Oak Harbor, WA). We attached PEEK tubing (Upchurch Scientific) into the fluidic access holes in the PCB using epoxy and made electrical connection with wires soldered into the PCB at one end and glued to gold bond pads at the other end using conductive epoxy (ITW Chemtronics, Kennesaw, GA). The molded PDMS die was manually aligned to the Pyrex die, covered with a glass slide for rigidity, and clamped using binder clips to form the enclosed channel structure.

Flow Setup. The flow into the channel is controlled by syringe pumps (KD Scientific 210C, Holliston, MA) as depicted in Figure 2. A four-way valve (V-101D, Upchurch Scientific) selects between water and detergent (0.1% Alconox) solution, each in a 10-mL Hamilton glass syringe (Hamilton Co., Reno, NV). Downstream, a second valve enables flow of particles into the device. For concentration enhancement experiments, a four-way valve is used in combination with a second syringe and a Becton-Dickinson plastic syringe (BD, Franklin Lakes, NJ). For characterization experiments, a six-port injection valve (V-450, Upchurch Scientific) is used with a sample loop to more accurately control sample volume.

Electrical Excitation. We generate electrical excitation using an Agilent 33250 signal generator (Agilent, Palo Alto, CA). Electrodes were excited with a 20-V_{pp}, 500-kHz sine wave for experiments with polystyrene microspheres and with a 40-V_{pp} 100-kHz sine wave for spores.

(17) Zhou, G.; Imamura, M.; Suehiro, J.; Hara, M. *Conf. Rec. IEEE Ind. Appl. Conf.* **2002**, *2*, 1404–1411.
(18) Lapizco-Encinas, B. H.; Simmons, B. A.; Cummings, E. B.; Fintschenko, Y. *Anal. Chem.* **2004**, *76*, 1571–1579.
(19) Lapizco-Encinas, B. H.; Davalos, R. V.; Simmons, B. A.; Cummings, E. B.; Fintschenko, Y. *J. Microbiol. Methods* **2005**, *62*, 317–326.
(20) Huang, Y.; Wang, X.-B.; Becker, F. F.; Gascoyne, P. R. C. *Biophys. J.* **1997**, *73*, 1118–1129.
(21) Li, H.; Zheng, Y.; Akin, D.; Bashir, R. *J. Microelectromech. Sysy.* **2005**, *14*, 103–112.
(22) Kentsch, J.; Durr, M.; Schnelle, T.; Gradl, G.; Muller, T.; Jager, M.; Normann, A.; Stelzle, M. *IEE Proc.: Nanobiotechnol.* **2003**, *150*, 82–89.
(23) Aldaeus, F.; Lin, Y.; Roeraade, J.; Amberg, G. *Electrophoresis* **2005**, *26*, 4252–4259.
(24) Stroock, A. D.; Dertinger, S. K.; Ajdari, A.; Mezic, I.; Stone, H. A.; Whitesides, G. M. *Science* **2002**, *295*, 647–651.

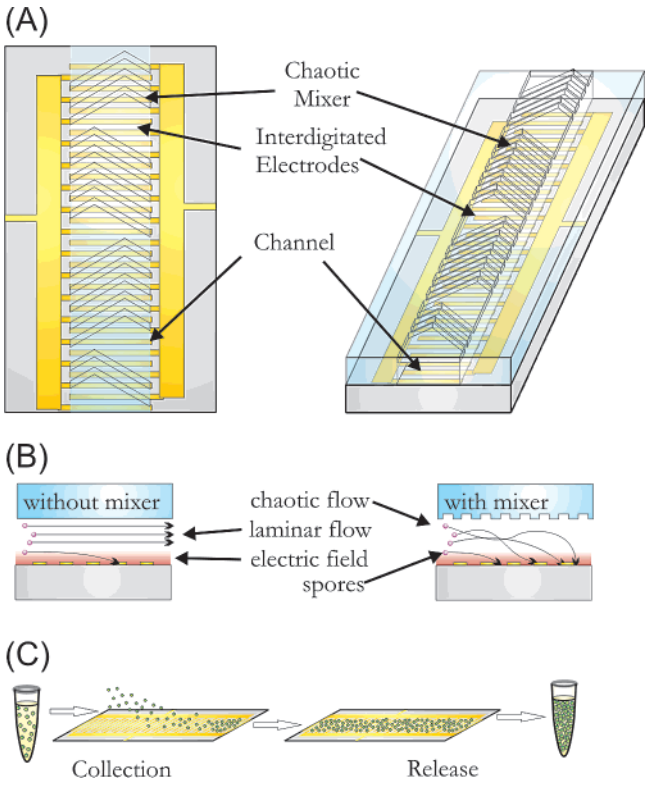

Figure 1. (A) Device overview, showing the chaotic mixer atop the interdigitated electrodes. (B) Schematic of effect of mixer on particle capture. By circulating the flow, the mixer brings more particles into proximity with the electrodes, enhancing concentration efficiency. (C) Overview of concentrator operation. By collecting particles, the concentrator delivers an output solution that has a higher particle concentration than the input solution.

Optics. Imaging was performed using a Zeiss Axioplan 2MOT upright microscope (Zeiss, Thornwood, NY) and a Sensicam QE cooled CCD digital camera (The Cooke Corp., Romulus, MI). A Cy3 fluorescence filter (41007a, Chroma, Rockingham, VT) was used for viewing microspheres, and a FITC fluorescence filter (41001, Chroma) was used for imaging spores.

Measuring Suspension Concentration. We measured bead and spore suspension concentrations using a NanoDrop ND-1000 spectrophotometer (NanoDrop Technologies, Wilmington, DE), which can measure 1−2-μL samples. We used absorbance at 600-nm wavelength for beads, and absorbance averaged from 400 to 600-nm wavelengths for spores. The detection threshold for both beads and spores is $\sim 3 \times 10^6$ particles/mL. We created a set of calibration curves using measurements of known bead and spore concentrations to correlate spectroscopic absorbance to sample concentration. One calibration curve was used for all bead experiments. For spore experiments, a new calibration curve was produced each time to account for variability in sample preparation procedures.

Measurement Protocol. We started experiments by flushing the channel with water at 500 μL/min to eliminate pockets of air in the mixer grooves. Next, we applied voltages to the electrodes and introduced the particle suspension into the channel at 500 (microspheres) or 100 μL/min (spores). This caused particles to be trapped on the electrodes due to pDEP. After trapping the desired volume of particle suspension, we introduced deionized water to remove particles from flow. To release particles, we introduced the detergent solution into the channel at 500 μL/min. We collected drops at the output into 0.2-mL PCR tubes, capped the tubes immediately to minimize evaporation, and measured sample concentrations using the spectrophotometer.

Modeling. Modeling was performed using our previously developed modeling software.[13] This software takes as inputs the electric field, obtained from an analytic solution,[25] dielectric properties of the particle and its surrounding medium, and other system parameters. Based on the resulting drag, dielectrophoretic, gravitational, and lift forces exerted on the particle, it computes the particle trajectory and thus determines whether a set of operating conditions enables the device to trap the particle. Since the electrical properties of spores have not been determined, we used a CM factor of 0.3 in all simulations; since we were only interested in trends, rather than absolute values, this was an acceptable approximation. We used a 0.5-μm particle radius, which agrees with published values for spore radii.[26]

RESULTS AND DISCUSSION

Concentrator Design. The concentrator consists of a microfluidic channel with interdigitated electrodes on the bottom and a staggered herringbone mixer[24] at the top (Figure 1A). The concentrator uses pDEP—pulling particles into the maximum electric field—to collect particles. One important assumption underlying our microconcentrator is that the liquid will be of sufficiently low conductivity (typically $<\sim$0.3 S/m) that pDEP can occur. In our case, this is a valid assumption because we are designing our microconcentrator to be downstream of a device that can provide liquid of known conductivity (e.g., air sampler). In other applications, such as monitoring of body fluids or ocean water, one would not be able to use pDEP.

The staggered herringbone mixer circulates the liquid in the channel, bringing particles to the trapping region of the electrodes (Figure 1B). As sample flows through the channel, the electrodes apply a downward force selectively to the particles, trapping them as they flow down the channel (Figure 3A). The surrounding liquid is not affected and is sent to waste. When enough particles have accumulated on the electrodes, the force is deactivated and the particles are resuspended into a smaller volume, thereby producing a concentrated sample (Figure 1C).

We first were interested in optimizing the interdigitated electrodes for particle capture. For this geometry, at a given voltage the downward DEP force increases proportionally with electrode dimension (electrode width and spacing = d), while the holding strength decreases as d increases. This tradeoff results in an optimal electrode geometry that minimizes capture distance for a given particle starting height, as shown in Figure 3B. Plotting this optimal geometry d against the starting height, we see that, to a first approximation, picking d equal to the expected starting height will minimize the trapping distance.

Interestingly, the optimal d is independent of applied flow rate (Figure 3C) as well as particle radius (not shown), at least to first order. Essentially, this is due to the fact that the forces affecting the particle trajectory scale equivalently with those parameters. For instance, in the case of particle radius R, both the buoyancy

(25) Chang, D. E.; Loire, S.; Mezic, I. *J. Phys. D: Appl. Phys.* **2003**, *36*, 3073−3078.
(26) Katz, A.; Alimova, A.; Xu, M.; Gottlieb, P.; Rudolph, E.; Steiner, J. C.; Alfano, R. R. *Opt. Lett.* **2005**, *30*, 589−591.

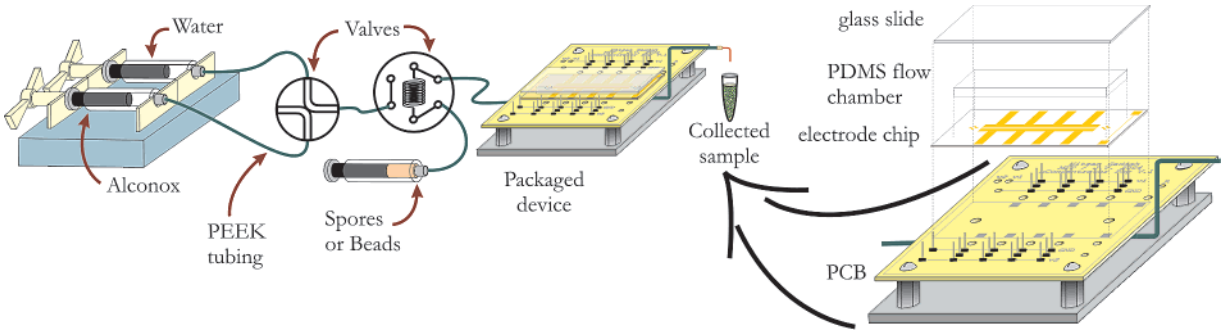

Figure 2. Packaging and flow setup.

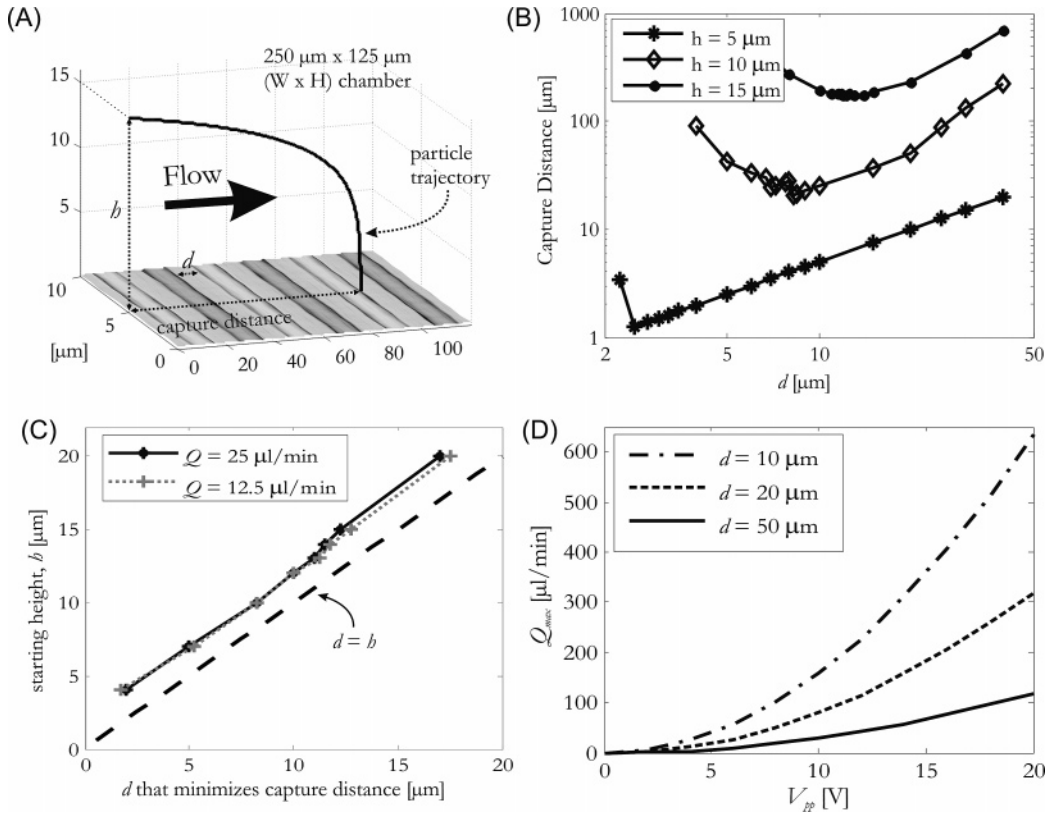

Figure 3. (A) Overview of simulations, showing how a particle initially at height *h* is drawn toward electrodes with width and spacing *d* and captured at some distance from the start. (B) Plots of the capture distance versus the electrode width/spacing *d* for different starting heights, showing that an optimal *d* exists for each starting height. (C) Starting height versus optimal *d* shows that the two are approximately equal irrespective of overall flow rate. (D) Holding of particles versus applied voltage for different electrode spacing *d*, showing the expected quadratic dependence on voltage and inverse dependence on *d*.

force and the *z*-directed DEP force scale as R^3 to first order. If we then form kinematic equations describing the particle trajectory, we find that upon minimizing that trajectory with respect to *d* the factors of *R* (and *Q*) will cancel. We emphasize that this does *not* imply that the capture distance is independent of *Q* or *R*; instead, we are stating that the electrode dimension that *minimizes* the capture distance is independent.

This latter result simplifies electrode design significantly. Given an initial height from which one wishes to capture, that height in turn dictates the electrode spacing. This will result in the smallest channel length and thus the smallest channel volume, resulting in the highest concentration enhancement. We point out that this optimal electrode dimension may not meet other requirements. For instance, we see in Figure 3B that the capture distance increases with increasing starting height; thus, trying to capture from a large starting height may require an impractically long channel.

Second, once captured, the particles need to be held against the fluid flow, and larger *d* results in a weaker holding force at constant voltage (Figure 3D). Since the maximum voltage is usually determined by the available electronics, the combination of maximum voltage and throughput requirements set an upper limit on *d*.

The choice of optimal electrode geometry is also coupled to the channel dimensions; for instance, decreasing the cross-sectional area will increase the drag force on particles at a given volumetric flow rate, requiring a smaller *d* to be able to hold particles at a given voltage. Thus, given a target flow rate of 500 μL/min, we chose a channel cross section large enough that we could capture beads in the channel at 20 V_{pp} (spores at 40 V_{pp})

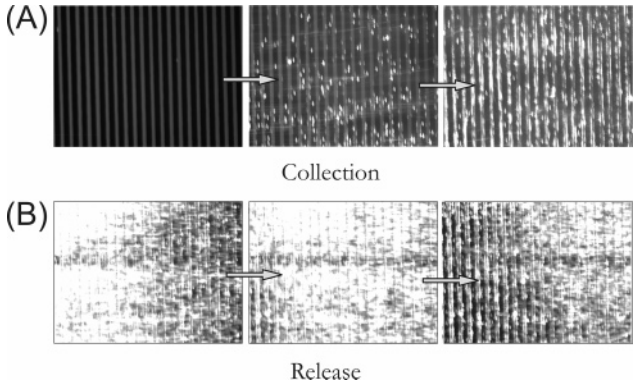

Figure 4. (A) Sequence of spore collection in the device. The time from the first to last image is ~15 s. (B) Initial spore release from the device, showing the increase in intensity as the spore plug flows past the field of view. The time from the first to last image is <1 s. Spores completely release after ~5 s (not shown).

but small enough that we could still mix most of the liquid in the channel using the chaotic mixer. Since published results[24] report mixing only in the center 50% of the channel cross-sectional area, we chose an electrode spacing/width of 10 μm for experiments with beads and 25 μm for spores in a channel of 250 × 100 μm.[24,27]

While interdigitated electrodes have been used repeatedly in the past to apply DEP forces to particles,[20,28] including for particle concentration,[21,29] there has not thus far been a report on the optimization of this geometry for concentration. In large part we are able to do this because of our quantitative modeling software,[12,13] which allows us to extract useful design parameters (e.g., release flowrates).

Device Operation. Upon introducing particles into a clean, energized device, both spores and beads collect on the electrodes (Figure 4A). Since we concentrate particles onto the electrodes, we were concerned that they would be irreversibly adsorbed and that removing the voltage would not be sufficient to release the particles. This is commonly observed in pDEP-based particle capture, and indeed, we observed that many particles did not release when we removed the voltage on an uncoated device (data not shown).

We addressed the problem of irreversible adsorption of particles to the surface using a combination of a surface modification and a release agent. We coated the electrode surface with Sylgard Prime Coat, which renders the chip surface hydrophobic, and used an anionic detergent (Alconox) to release particles into the flow. Detergents disrupt interactions between the particles and the surface, enabling the particles to release from the surface more easily. Using detergent has an additional advantage in that it eliminates the need to turn off the voltage for particle release, eliminating the need to perfectly synchronize the voltage turnoff with the detergent solution entering the channel. Since pDEP relies upon the presence of a low-conductivity medium, introducing the detergent solution, which is anionic and hence increases solution conductivity (from ~5×10^{-4} to ~10^{-1} S/m), switches the concentrator to nDEP operation. Both this switch from pDEP to nDEP and the intrinsic destabilizing action of a detergent results in efficient particle release for both beads and spores. Importantly, we found that using a high-conductivity buffer or simply turning off the electrodes was not sufficient to fully release particles from the chip, suggesting that the detergent solution was disrupting particle/surface interactions and not simply switching from pDEP to nDEP.

Detergents are known to lyse cells and other bioparticles. However, evidence in the literature suggests that spores are resistant to detergents.[30] We verified that spores are not adversely affected by first suspending them in detergent solution for 30 min and then resuspending them in DI water by dialysis. We were able to restain and visualize the spores in both fluorescence and bright-field illumination (data not shown). We used bright-field images to extract the spore radii, whose values agreed well with published values (data not shown).

This use of a detergent takes advantage of the robustness of spores, which is the particle we are interested in concentrating. Detergent use could pose some limitations in other applications, however. If the concentrated particle is susceptible to detergent lysis and intact particles are required at the detector, then a different release method would be required. If, however, the detector only required intracellular biomolecules, then detergent lysis during release could be an advantage.

Concentration Enhancement. The challenge in assessing the performance of microscale concentrators lies in accurately obtaining the small liquid volumes created by the devices and making concentration measurements in those small volumes. For example, the internal volume of our microconcentrator is 0.5 μL, which is both difficult to extract and mismatched to the volumes required for most commercial instruments capable of measuring particle concentrations (e.g., Coulter counter, hemacytometer, spectrophotometer). Other reports on microscale concentrators monitor the concentration process on-chip by imaging fluorescence of the captured particles[18] or measuring impedance changes at the electrodes.[29]

Instead, we wanted a measurement of the practical, or extrinsic, concentration enhancement, including the challenge of actually removing the concentrated sample from the device. Our solution was to collect drops (limited to a minimum of ~10 μL each) from the outlet of the device and measure the concentration of particles in each of those drops using a commercial UV spectrophotometer specifically developed to measure in 1−2-μL volumes (see Materials and Methods). We defined an extrinsic concentration enhancement as the [maximum measured output concentration]/[input concentration]. This value is a conservative attempt to estimate the attainable concentration enhancement.

Extrinsic concentration enhancement measures not only the performance of the device but also includes factors such as Taylor dispersion, the finite time to release the spores, and the relatively large drops that are formed at the outlet tubing. Since these factors can all be improved or avoided (e.g., direct coupling to a detector to avoid having to form drops), we defined a measure of the intrinsic performance of the mixer. Intrinsic concentration enhancement describes the maximum achievable enhancement and disregards any extrinsic effects. We define intrinsic concentration enhancement as [number of particles released]/[channel volume],

(27) Stroock, A. D.; McGraw, G. J. *Philos. Trans. R. Soc. London, Ser. A* **2004**, *362*, 971−986.
(28) Albrecht, D. R.; Sah, R. L.; Bhatia, S. N. *Biophys. J.* **2004**, *87*, 2131−2147.
(29) Suehiro, J.; Hamada, R.; Noutomi, D.; Shutou, M.; Hara, M. *J. Electrost.* **2003**, *57*, 157−168.
(30) Young, S. B.; Setlow, P. *J. Appl. Microbiol.* **2004**, *96*, 289−301.

where the number of released particles is calculated by integrating under the output concentration curves.

Figure 5 shows typical output concentration curves for beads (Figure 5A) and *B. subtilis* spores (Figure 5B). We have been able to repeatably achieve extrinsic concentration enhancements up to ~40× using beads and up to ~9× using *B. subtilis* spores. These results correspond to intrinsic concentrations enhancements of 750−1500× for beads and 350−1000× for spores (depending on the actual drop volume).

Using beads, we characterized the extrinsic concentration enhancement as we varied input particle number. To ease the experiments, we kept the particle concentration constant and varied input volume. We used small volumes of beads at relatively high concentration (6×10^7/mL) to minimize experiment time. The results show the trends of the device performance with varying input volumes (Figure 5C). For an intermediate range of inputs, the output concentration varies proportionally to the input number of beads. When the input exceeds this intermediate range, the finite trapping area (that is, the area of the bottom of the channel) sets a limit on the number of particles that can be trapped and, thus, on the output concentration. This causes the output concentration to saturate at a value corresponding to the maximum number of particles that can be trapped. At the low range of input volume, the resulting output concentration is below the measurement detection threshold and the output does not appear to change with variations in the input.

Figure 5C also shows a comparison between results obtained with and without the use of a chaotic mixer. As expected, use of the chaotic mixer increases the concentration enhancement in the intermediate range. This is likely due to the mixer circulating particles and bringing them closer to the electrodes as shown in Figure 1B. At larger input volumes, the electrodes saturate with and without the mixer, causing the two curves to overlap. Thus, the mixer is useful for high-throughput microconcentrators because it effectively permits the electric field to sample a larger volume of fluid, allowing us to increase the cross-sectional area. We are further studying the properties of these mixers to optimize their geometry for these applications.[31]

We note that the peak output concentration in Figure 5C remains at or below the input particle concentration, pointing to the relative inefficiency of the device. Our design is currently optimized for throughput (volume/time), not trapping efficiency (number of particles captured/ number of particles input). This combines with the fact that Figure 5C measures extrinsic concentration to give an ~1× extrinsic concentration enhancement at high input volumes (but still a ≫1× intrinsic concentration enhancement). The primary reason for the difference between Figure 5A,B and Figure 5C is that we used a lower input concentration and larger volume for Figure 5A,B. To minimize experimental time, we increased the input concentration for the experiments in Figure 5C and decreased the volume. Since increasing the input concentration increases the denominator in the extrinsic concentration enhancement relation, the extrinsic concentration enhancement will naturally decrease. This, however, does not change the fundamental result of Figure 5C, which is that the mixer improves the efficiency of the concentrator.

(31) Lee, H.-Y.; Voldman, J., in preparation. 2006.

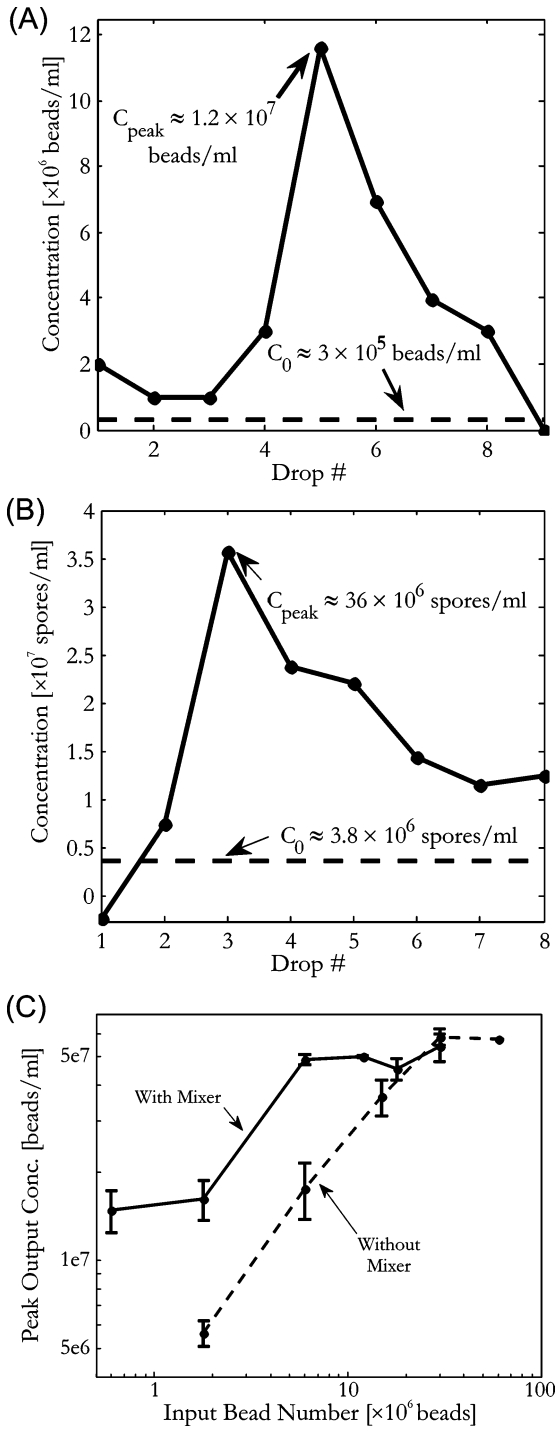

Figure 5. Measured output concentration curves with (A) beads and (B) spores. We measured the particle concentration in each collected drop and compared that to the known input concentration (C_0). Beads were concentrated at a flow rate of 500 μL/min, while spores were collected at 100 μL/min and released at 500 μL/min. Peak concentration enhancement (C_{peak}) is ~40×, while for spores it is ~9×. (C) Concentration enhancement of beads with (—) and without (---) mixer. We flowed in various input volumes at 500 μL/min while keeping the input bead concentration (6×10^7 beads/mL) constant, thus varying the input particle number. At low input particle numbers, the concentration enhancement is below the detection threshold. With increasing particle number, the peak output concentration rises and then saturates at high-input particle number. Use of the chaotic mixer increases the concentration enhancement at a given input particle number.

Together our results demonstrate the successful operation of the concentrator as well as characterization of its performance. We have focused on operation at high throughput, rather than high capture efficiency or high concentration enhancement, reasoning that only throughputs approaching approximately milliliters per minute would ultimately be useful. Of course, one benefit of microfabrication is the potential to combine multiple devices in parallel to further increase throughput.

CONCLUSIONS

We have presented modeling and results of a microfluidic device optimized for concentrating particles at high throughput. By combining interdigitated electrodes with a chaotic mixer, we created a concentrator that was simple to fabricate yet effective. Our modeling indicated that there is an optimal interdigitated electrode geometry for collecting particles when throughput is the primary concern, which is that the electrode width and spacing should be approximately equal to the maximum starting height of the particles. We introduced an approach to releasing particles from electrodes using a combination of detergent and release layer. Finally, we demonstrated operation with both beads and spores, attaining up to ~40× extrinsic concentration enhancement of beads at 500 μL/min and up to ~9× extrinsic concentration enhancement of *B. subtilis* spores at 100 μL/min.

ACKNOWLEDGMENT

We acknowledge Brian Taff for initial development of the packaging and Mike Vahey for helpful discussions. This work was partially supported by Draper Laboratories and a Siebel Fellowship (N.G.).

Received for review June 28, 2006. Accepted September 7, 2006.

AC061170I